

Platinum Metal Complexes of Mixed Thia/Oxa Ionophores. The Synthesis and Single-crystal X-Ray Structures of $[\text{Pd}([\text{15}] \text{aneS}_2\text{O}_3)_2][\text{PF}_6]_2$ and $[\text{RuCl}(\text{PPh}_3)([\text{15}] \text{aneS}_2\text{O}_3)_2]\text{PF}_6 \cdot \text{H}_2\text{O}$ ($[\text{15}] \text{aneS}_2\text{O}_3 = 1,4,7\text{-trioxa-10,13-dithiacyclopentadecane}$) †

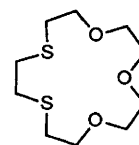
Alexander J. Blake, Gillian Reid, and Martin Schröder*

Department of Chemistry, University of Edinburgh, West Mains Road, Edinburgh EH9 3JJ

The synthesis and characterisation of a series of mixed thia/oxa donor macrocyclic complexes *cis*- $[\text{MCl}_2([\text{15}] \text{aneS}_2\text{O}_3)]$, $[\text{M}([\text{15}] \text{aneS}_2\text{O}_3)_2]^{2+}$ ($\text{M} = \text{Pd}$ or Pt), $[\text{MCl}_2([\text{15}] \text{aneS}_2\text{O}_3)_2]^+$ ($\text{M} = \text{Rh}$ or Ir), and $[\text{RuCl}(\text{PPh}_3)([\text{15}] \text{aneS}_2\text{O}_3)_2]^+$ ($[\text{15}] \text{aneS}_2\text{O}_3 = 1,4,7\text{-trioxa-10,13-dithiacyclopentadecane}$) are described. Reaction of MCl_2 ($\text{M} = \text{Pd}$ or Pt) with one molar equivalent of $[\text{15}] \text{aneS}_2\text{O}_3$ affords the complex *cis*- $[\text{MCl}_2([\text{15}] \text{aneS}_2\text{O}_3)]$; addition of a second equivalent affords the bis complex cations $[\text{M}([\text{15}] \text{aneS}_2\text{O}_3)_2]^{2+}$. The complex $[\text{Pd}([\text{15}] \text{aneS}_2\text{O}_3)_2][\text{PF}_6]_2$ crystallises in the monoclinic space group $P2_1/c$, $a = 10.394(4)$, $b = 14.003(4)$, $c = 11.675(5)$ Å, $\beta = 104.22(3)$, $U = 1647$ Å³, and $Z = 2$. The single-crystal X-ray structure shows the Pd^{II} occupying a crystallographic inversion centre, with square-planar co-ordination by the $[\text{15}] \text{aneS}_2\text{O}_3$ ionophores through the thioether S-donors, $\text{Pd-S}(1) 2.314 9(10)$, $\text{Pd-S}(4) 2.301 7(10)$ Å. The O-donors point away from the Pd^{II} to give a relatively flattened complex. Reaction of $\text{MCl}_3 \cdot 3\text{H}_2\text{O}$ ($\text{M} = \text{Rh}$ or Ir) with two molar equivalents of $[\text{15}] \text{aneS}_2\text{O}_3$ affords the complex cations $[\text{MCl}_2([\text{15}] \text{aneS}_2\text{O}_3)_2]^+$. Treatment of $[\text{RuCl}_2(\text{PPh}_3)_3]$ with two molar equivalents of $[\text{15}] \text{aneS}_2\text{O}_3$ gives the complex cation $[\text{RuCl}(\text{PPh}_3)([\text{15}] \text{aneS}_2\text{O}_3)_2]^+$. The complex $[\text{RuCl}(\text{PPh}_3)([\text{15}] \text{aneS}_2\text{O}_3)_2]\text{PF}_6 \cdot \text{H}_2\text{O}$ crystallises in the orthorhombic space group $Pbcn$, $a = 19.252 6(14)$, $b = 25.968(3)$, $c = 18.903 3(23)$ Å, $U = 9451$ Å³, and $Z = 8$. The single-crystal X-ray structure shows octahedral co-ordination at Ru^{II} with the Cl^- and PPh_3 ligands mutually *trans*, $\text{Ru-Cl} 2.458(3)$, $\text{Ru-P} 2.319(3)$ Å. The $[\text{15}] \text{aneS}_2\text{O}_3$ ligands are bound exocyclically to Ru^{II} via four thioether S-donors, $\text{Ru-S} 2.390(3)$, $2.394(3)$, $2.395(3)$, $2.405(3)$ Å. The O-donors of $[\text{15}] \text{aneS}_2\text{O}_3$ are not bound to the metal centre but, unlike the complex $[\text{Pd}([\text{15}] \text{aneS}_2\text{O}_3)_2]^{2+}$, are directed towards the face occupied by the Cl^- ligand and away from the sterically bulky PPh_3 ligand. The $[\text{15}] \text{aneS}_2\text{O}_3$ ligands in $[\text{RuCl}(\text{PPh}_3)([\text{15}] \text{aneS}_2\text{O}_3)_2]^+$ therefore form a cavity at one face of the metal centre in which the co-ordinated Cl^- ligand sits.

Macrocyclic ligands incorporating recognition sites capable of binding both hard- and soft-metal guest ions are of considerable current interest since they may facilitate electron-transfer processes and serve as models of relevance to biological processes.¹⁻⁵ They may also provide effective systems with which to monitor alkali-metal concentrations in solution, due to the allosteric effect of binding two metal ions in close proximity to each other.²⁻⁵ One approach utilising ferrocene derivatives, which show highly reversible $\text{Fe}^{\text{II}}\text{-Fe}^{\text{III}}$ couples, as potential sensors for substrate cations, is well established.^{3,4} For example, it has been shown recently that the binding of Li^+ to aza-15-crown-5 (1,4,7,10-tetraoxa-13-azacyclopentadecane, $[\text{15}] \text{aneNO}_4$) covalently attached to a ferrocene moiety results in a shift in the $\text{Fe}^{\text{II}}\text{-Fe}^{\text{III}}$ couple to more anodic potentials.³ Green and co-workers⁵ have adopted an alternative approach, using dithiolate donors incorporated in the side chains of crown ethers to attach the ionophore to $[\text{M}(\eta^5\text{-C}_5\text{H}_5)_2]^{2+}$ ($\text{M} = \text{Mo}$ or W) fragments.

We have been investigating the co-ordination chemistry of homoleptic thioether crowns,⁶ and proposed that mixed thioether/oxaether crowns would bind soft second- and third-row metal ions via the S-donors, leaving the O-donors unco-ordinated and therefore available for binding to Main Group 1 and 2 ions, amino acids, or related cations/anions. However, this approach necessitates *exo* co-ordination of transition-metal ions to the macrocyclic ring since *endo* co-ordination would block guest co-ordination via the O-donors. Co-ordination of



$[\text{15}] \text{aneS}_2\text{O}_3$

transition-metal ions *exo* to a thioether crown has been noted,^{7,8} and indeed this is proposed as the first step in co-ordination, since the metal-free thioether crowns typically adopt conformations in which the S-donors lie in *exo* positions.^{8,9} However, *exo* complexes are not stabilised by the macrocyclic effect, only by chelate formation. In addition, monodentate thioethers are often kinetically labile, particularly with first-row metal centres.¹⁰ We therefore undertook a preliminary investigation into the co-ordination chemistry of $[\text{15}] \text{aneS}_2\text{O}_3$ to determine whether this simple ionophore would form stable platinum-metal complexes via chelation of the two thioether S-donors. We describe herein the synthesis of a series of complexes of $[\text{15}] \text{aneS}_2\text{O}_3$ with the platinum-metal ions Pd^{II} , Pt^{II} , Rh^{III} , Ir^{III} , and Ru^{II} .

† Supplementary data available: see Instructions for Authors, *J. Chem. Soc., Dalton Trans.*, 1990, Issue 1, pp. xix-xxii.

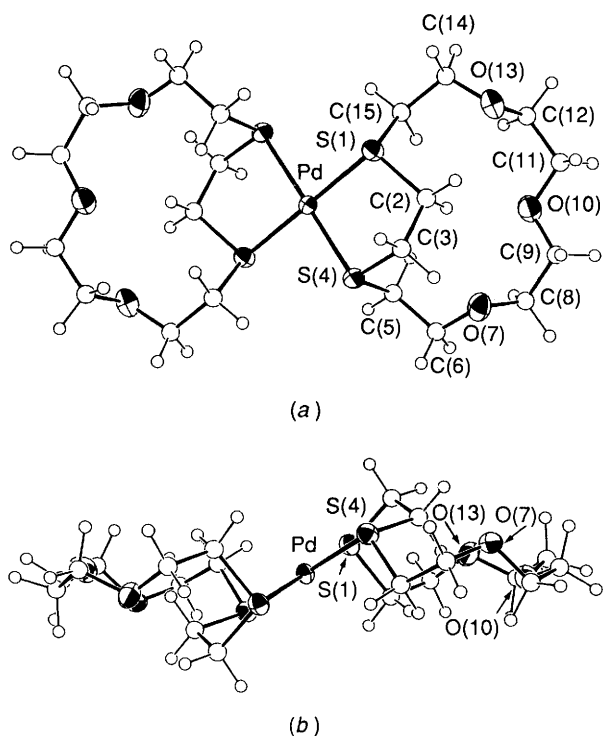


Figure 1. Single crystal X-ray structure of $[\text{Pd}([\text{15]aneS}_2\text{O}_3)_2]^{2+}$. Two views (a) and (b) with numbering scheme adopted

The synthesis of a series of mixed polythia/oxa macrocycles has been reported by Bradshaw and co-workers.^{11–13} The general procedure involves a high-dilution cyclisation of the appropriate oligoethylene glycol dichloride with ethane-1,2-dithiolate. The single-crystal X-ray structure of $[\text{15]aneS}_2\text{O}_3$ shows the S atoms lying in *exo* positions with respect to the macrocyclic ring with an S–C–C–S torsion angle of $-166.8(3)^\circ$. The two S atoms are about 4.5 Å apart and *anti* with respect to each other.¹⁴ Since the discovery of crown ethers by Pedersen^{15,16} the selectivity of these systems and their derivatives for alkali-metal cation complexation and transport has received a great deal of attention.^{17,18} Izatt *et al.*¹⁹ have demonstrated that partial substitution of O-donor atoms by sulphur changes the cation selectivity pattern. Thus, the stability of Group 1 and 2 metal complexes decreases while the affinity of the ionophores for Ag^+ and Hg^{2+} through S-binding is enhanced. A similar increased affinity for platinum-metal ions might be expected.

Few examples of transition metal complexes of mixed O/S-donor macrocycles have been reported. The complex *cis*- $[\text{PdCl}_2(\text{L})]$ (L = 1,4,10,13-tetraoxa-7,16-dithiacyclo-octadecane) incorporates Pd^{II} bound to the two thioether S-donors; however, since the S-donors are at 1,10- as opposed to 1,4-positions, the conformation of the co-ordinated ionophore is not pre-organised for guest complexation.²⁰ Our interests in the co-ordination chemistry of $[\text{15]aneS}_2\text{O}_3$ lay initially in the elucidation of structures of the resulting complexes and in the conformation(s) of the co-ordinated macrocycle around metal ions which would show highly reversible redox behaviour.

Results and Discussion

Palladium.—Treatment of PdCl_2 with one molar equivalent of $[\text{15]aneS}_2\text{O}_3$ in refluxing $\text{MeOH-H}_2\text{O}$ affords a bright yellow solution. Removal of the solvent *in vacuo* gives an

orange residue which can be recrystallised from EtOH. The fast-atom bombardment (f.a.b.) mass spectrum of the product shows a molecular-ion peak with the correct isotopic distribution at m/z 357 corresponding to $[\text{106Pd}([\text{15]aneS}_2\text{O}_3) - \text{H}]^+$. The ^1H n.m.r. spectrum of the complex shows a second-order multiplet in the range δ 2.28–4.18, while the ^{13}C DEPT n.m.r. spectrum shows five distinct methylene C resonances at 71.07, 70.33, 69.38 (CH_2O), 37.64, and 35.73 p.p.m. (CH_2S). These values are shifted relative to those found for the free $[\text{15]aneS}_2\text{O}_3$ ligand (δ 72.09, 70.46, 69.23, 32.18, and 30.58 p.p.m.). The u.v.-visible spectrum of the product reveals absorption bands at $\lambda_{\text{max.}}$ = 394 nm ($\epsilon_{\text{max.}}$ = $975 \text{ dm}^3 \text{ mol}^{-1} \text{ cm}^{-1}$) and 262 (8 820) assigned to *d-d* and charge-transfer ($\text{S} \rightarrow \text{M}$ or $\text{Cl} \rightarrow \text{M}$) transitions respectively. The i.r. spectrum of the complex shows peaks at 340 and 320 cm^{-1} assigned to the Pd–Cl stretching vibrations, $\nu(\text{Pd-Cl})$, of a *cis*-dichloro complex; this assignment is complicated by the possible occurrence of Pd–S stretching vibrations in the same region of the spectrum. These data, together with elemental analyses, confirm the product as *cis*- $[\text{PdCl}_2([\text{15]aneS}_2\text{O}_3)]$.

Reaction of *cis*- $[\text{PdCl}_2([\text{15]aneS}_2\text{O}_3)]$ with one, or of PdCl_2 with two molar equivalents of $[\text{15]aneS}_2\text{O}_3$ in refluxing $\text{MeOH-H}_2\text{O}$ affords a bright yellow solution. Addition of an excess of NH_4PF_6 gives a yellow precipitate which can be recrystallised from MeNO_2 . The corresponding BPh_4^- salt can be isolated by using NaBPh_4 instead of NH_4PF_6 . However, attempted recrystallisation of the BPh_4^- salt from Me_2CO , MeCN , MeNO_2 , or dimethyl sulphoxide (dmsO) resulted in its rapid decomposition to a black residue. The f.a.b. mass spectrum of the complex reveals molecular ion peaks with the correct isotopic distributions at m/z 610 and 358 corresponding to $[\text{106Pd}([\text{15]aneS}_2\text{O}_3)_2]^+$ and $[\text{106Pd}([\text{15]aneS}_2\text{O}_3)]^+$ respectively. The ^1H n.m.r. spectrum exhibits a series of multiplets centred at δ 3.96, 3.62, and 3.35 due to the protons of co-ordinated $[\text{15]aneS}_2\text{O}_3$. The ^{13}C DEPT n.m.r. spectrum shows resonances assigned to methylene C centres at 69.99, 68.84, 68.15 (CH_2O), and 37.11 p.p.m. (two overlapping resonances due to CH_2S) suggesting that the two macrocycles are equivalent in solution. This, combined with microanalytical and i.r., and u.v.-visible spectral data, confirms the formulation $[\text{Pd}([\text{15]aneS}_2\text{O}_3)_2][\text{PF}_6]_2$ for this complex.

In order to establish the conformation of the co-ordinated macrocycles, a single-crystal X-ray structure determination of the complex was undertaken. The structure of $[\text{Pd}([\text{15]aneS}_2\text{O}_3)_2][\text{PF}_6]_2$ shows [Figure 1(a) and (b)] the Pd^{II} ion occupying a crystallographic inversion centre and bound through the four thioether S-donors of two co-ordinated $[\text{15]aneS}_2\text{O}_3$ ligands, Pd–S(1) 2.314 9(10), Pd–S(4) 2.301 7(10) Å, S(1)–Pd–S(4) $89.78(4)^\circ$. As anticipated, all the O-donors are directed away from the Pd^{II} and do not interact with it. A general feature of homoleptic thioether macrocyclic co-ordination with Pd^{II} is the long-range apical interaction with fifth and sixth S-donor atoms;²¹ this clearly does not occur with the corresponding O-donors.

Platinum.—The platinum(II) complexes *cis*- $[\text{PtCl}_2([\text{15]aneS}_2\text{O}_3)]$ and $[\text{Pt}([\text{15]aneS}_2\text{O}_3)_2][\text{PF}_6]_2$ have been prepared by similar routes to the Pd^{II} analogues.

The f.a.b. mass spectrum of $[\text{PtCl}_2([\text{15]aneS}_2\text{O}_3)]$ shows molecular-ion peaks with the correct isotopic distribution at m/z 483 and 447 corresponding to $[\text{195Pt}^{35}\text{Cl}([\text{15]aneS}_2\text{O}_3) + \text{H}]^+$ and $[\text{193Pt}([\text{15]aneS}_2\text{O}_3)]^+$ respectively. The ^1H n.m.r. spectrum shows a second-order multiplet in the range δ 2.83–4.30 assigned to the macrocyclic protons, while the ^{13}C DEPT n.m.r. spectrum shows five resonances assigned to the methylene C resonances at 70.70, 70.59, 69.60 (CH_2O), 37.85, and 35.86 p.p.m. (CH_2S). The i.r. spectrum of the complex shows peaks at 330 and 310 cm^{-1} assigned to the Pt–Cl

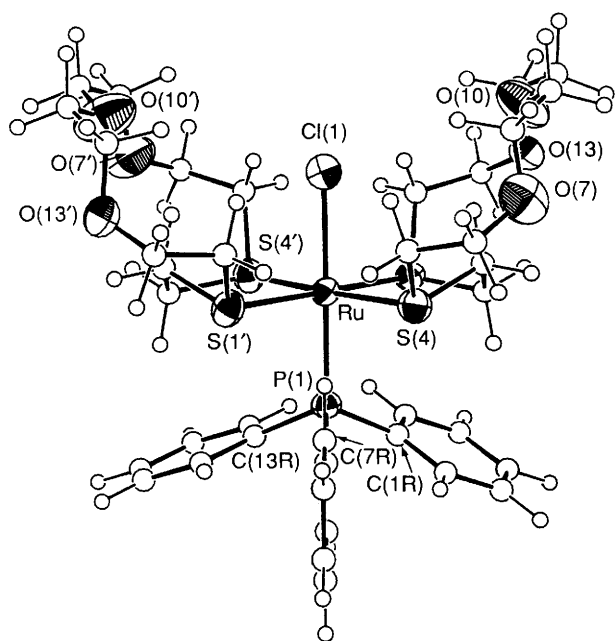


Figure 2. Single crystal X-ray structure of $[\text{RuCl}(\text{PPh}_3)([\text{15}] \text{aneS}_2\text{O}_3)_2]^+$ with numbering scheme adopted

stretching vibrations, $\nu(\text{Pt}-\text{Cl})$, of a *cis*-dichloro complex. Together with elemental analytical data, this confirms the product as *cis*- $[\text{PtCl}_2([\text{15}] \text{aneS}_2\text{O}_3)]$.

The f.a.b. mass spectrum of $[\text{Pt}([\text{15}] \text{aneS}_2\text{O}_3)_2][\text{PF}_6]_2$ exhibits molecular-ion peaks with the correct isotopic distribution at m/z 699 and 446 assigned to $[\text{195}\text{Pt}([\text{15}] \text{aneS}_2\text{O}_3)_2]^+$ and $[\text{195}\text{Pt}([\text{15}] \text{aneS}_2\text{O}_3) - \text{H}]^+$ respectively. The ^1H n.m.r. spectrum of the complex (δ 3.2–4.2), and the ^{13}C DEPT n.m.r. spectrum [70.17, 69.33, 69.00 (CH_2O), 37.57, and 36.86 p.p.m. (CH_2S)] are consistent with the formulation $[\text{Pt}([\text{15}] \text{aneS}_2\text{O}_3)_2][\text{PF}_6]_2$. This, together with microanalytical, u.v.–visible and i.r. spectral data, suggests that $[\text{Pt}([\text{15}] \text{aneS}_2\text{O}_3)_2]^{2+}$ adopts a structure very similar to that of $[\text{Pd}([\text{15}] \text{aneS}_2\text{O}_3)_2]^{2+}$, with square-planar co-ordination of Pt^{II} to four thioether S-donors with the O-donors directed well away from and not interacting with the metal ion.

Rhodium.—Treatment of $\text{RhCl}_3 \cdot 3\text{H}_2\text{O}$ with two molar equivalents of $[\text{15}] \text{aneS}_2\text{O}_3$ in refluxing MeOH gives a bright yellow solution. Addition of an excess of NH_4PF_6 yields an orange precipitate which can be recrystallised from MeNO_2 .

The f.a.b. mass spectrum of the complex shows molecular ion peaks with the correct isotopic distribution at m/z 677 and 642 corresponding to $[\text{103}\text{Rh}^{35}\text{Cl}_2([\text{15}] \text{aneS}_2\text{O}_3)_2]^+$ and $[\text{103}\text{Rh}^{35}\text{Cl}([\text{15}] \text{aneS}_2\text{O}_3)_2]^+$ respectively. The ^1H n.m.r. spectrum of the complex shows a second-order multiplet in the range δ 2.67–4.30 due to methylene protons, and the ^{13}C DEPT n.m.r. spectrum shows five absorption methylene C resonances at 69.55, 69.40, 67.85 (CH_2O), 36.59, and 33.53 p.p.m. (CH_2S), indicating that only one isomer is present in solution. Two absorption bands at $\lambda_{\text{max.}} = 435 \text{ nm}$ ($\epsilon_{\text{max.}} = 132 \text{ dm}^3 \text{ mol}^{-1} \text{ cm}^{-1}$) and 283 (32 970) are apparent in the u.v.–visible spectrum of the complex. The former is assigned to a *d-d* transition; the magnitude of the absorption coefficient for this band is comparable to that found for *trans*- $[\text{RhCl}_2([\text{16}] \text{aneS}_4)]^{2+}$ and suggests a *trans*-dichloro formulation for the product; related *cis*-dichloro complexes tend to exhibit considerably higher absorption coefficients than their *trans* analogues.²³ The i.r. spectrum of the complex shows a single peak at 350 cm^{-1} assigned to a Rh–Cl stretching

vibration, $\nu(\text{Rh}-\text{Cl})$, confirming the assignment of the product as *trans*- $[\text{RhCl}_2([\text{15}] \text{aneS}_2\text{O}_3)_2]\text{PF}_6$.

Iridium.—The iridium(III) complex *trans*- $[\text{IrCl}_2([\text{15}] \text{aneS}_2\text{O}_3)_2]\text{PF}_6$ can be prepared by reaction of $\text{IrCl}_3 \cdot 3\text{H}_2\text{O}$ with two molar equivalents of $[\text{15}] \text{aneS}_2\text{O}_3$ in refluxing MeOH. The f.a.b. mass spectrum of the complex shows molecular-ion peaks with the correct isotopic distribution at m/z 767, 733, 696, and 444 corresponding to $[\text{193}\text{Ir}^{35}\text{Cl}_2([\text{15}] \text{aneS}_2\text{O}_3)_2]^+$, $[\text{193}\text{Ir}^{35}\text{Cl}([\text{15}] \text{aneS}_2\text{O}_3)_2 + \text{H}]^+$, $[\text{193}\text{Ir}([\text{15}] \text{aneS}_2\text{O}_3)_2 - \text{H}]^+$, and $[\text{193}\text{Ir}([\text{15}] \text{aneS}_2\text{O}_3) - \text{H}]^+$ respectively. The ^1H (δ 3.3–4.2) and ^{13}C DEPT [69.68, 69.54, 67.57 (CH_2O), 35.76, and 32.60 p.p.m. (CH_2S)] n.m.r. spectra of *trans*- $[\text{IrCl}_2([\text{15}] \text{aneS}_2\text{O}_3)_2]^+$ confirm the presence of one symmetrical isomer in solution. The microanalytical and i.r., and u.v.–visible spectral data are also consistent with the formulation of the isolated product as *trans*- $[\text{IrCl}_2([\text{15}] \text{aneS}_2\text{O}_3)_2]\text{PF}_6$.

Ruthenium.—Treatment of $[\text{RuCl}_2(\text{PPh}_3)_3]$ with two molar equivalents of $[\text{15}] \text{aneS}_2\text{O}_3$ in refluxing MeOH affords a yellow solution. Addition of an excess of NH_4PF_6 gives a yellow precipitate which can be recrystallised from CH_2Cl_2 . The f.a.b. mass spectrum of the complex shows molecular ion peaks with the correct isotopic distributions at m/z 1 046, 904, 650, and 640 corresponding to $[\text{102}\text{Ru}^{35}\text{Cl}(\text{PPh}_3)([\text{15}] \text{aneS}_2\text{O}_3)_2\text{PF}_6 - 2\text{H}]^+$, $[\text{102}\text{Ru}^{35}\text{Cl}(\text{PPh}_3)([\text{15}] \text{aneS}_2\text{O}_3)_2 + \text{H}]^+$, $[\text{102}\text{Ru}^{35}\text{Cl}(\text{PPh}_3)([\text{15}] \text{aneS}_2\text{O}_3) - \text{H}]^+$, and $[\text{102}\text{Ru}^{35}\text{Cl}([\text{15}] \text{aneS}_2\text{O}_3)_2 - \text{H}]^+$ respectively. The ^1H n.m.r. spectrum of this species shows a multiplet at δ 7.3–8.0 assigned to the aromatic protons of PPh_3 . Further complex multiplets are observed at δ 2.0–4.3 due to the protons of $[\text{15}] \text{aneS}_2\text{O}_3$. A stoichiometry of 1 PPh_3 :2 $[\text{15}] \text{aneS}_2\text{O}_3$ is confirmed by integration of these signals. The ^{13}C DEPT n.m.r. spectrum shows, in addition to CH resonances due to the phenyl C centres of PPh_3 , four distinct resonances at 69.36, 68.54 (two overlapping) (CH_2O), 32.04, and 30.56 p.p.m. (CH_2S) assigned to methylene C centres of $[\text{15}] \text{aneS}_2\text{O}_3$. This, together with microanalytical and i.r., and u.v. visible spectral data, suggests the formulation $[\text{RuCl}(\text{PPh}_3)([\text{15}] \text{aneS}_2\text{O}_3)_2]\text{PF}_6$ for the complex.

In order to determine whether this complex was a *cis* or *trans* isomer and also to establish the conformation of the co-ordinated macrocycles, a single-crystal X-ray structure determination was undertaken. The crystal structure of $[\text{RuCl}(\text{PPh}_3)([\text{15}] \text{aneS}_2\text{O}_3)_2]^+$ shows (Figure 2) Ru^{II} bound octahedrally to all four thioether S-donors of two $[\text{15}] \text{aneS}_2\text{O}_3$ ligands, Ru–S(1) 2.394(3), Ru–S(1') 2.390(3), Ru–S(4) 2.395(3), Ru–S(4') 2.405(3) Å, with the Cl[−] and PPh_3 ligands occupying mutually *trans* positions, Ru–Cl(1) 2.458(3), Ru–P(1) 2.319(3) Å. The most interesting aspect of this structure is the conformation adopted by the polyoxa linkages of the co-ordinated $[\text{15}] \text{aneS}_2\text{O}_3$ ligands. The steric bulk of the PPh_3 ligand forces the non-bonded O-donors of the two $[\text{15}] \text{aneS}_2\text{O}_3$ ligands away from PPh_3 towards the face occupied by the Cl[−] ligand to form a partial cavity around Cl[−]. One water solvent molecule is associated with each cation and is disordered between two mutually incompatible sites. In one of these sites the water molecule is H-bonded to an O atom of one of the $[\text{15}] \text{aneS}_2\text{O}_3$ ligands [O(2S) \cdots O(13') 3.08(4) Å].

Electrochemistry.—Cyclic voltammetry of $[\text{Pd}([\text{15}] \text{aneS}_2\text{O}_3)_2][\text{PF}_6]_2$ in MeCN (0.1 mol dm^{-3} $\text{NBu}_4^+\text{PF}_6^-$) at platinum electrodes shows two irreversible reductions at $E_{\text{pc}} = -0.75$ and $-1.20 \text{ V vs. ferrocene-ferrocenium}$ at a scan rate of 200 mV s^{-1} . No oxidative activity is observed within the range of the solvent up to +2.0 V. The redox couples for this complex vary with both temperature and scan rate and would therefore not be useful for the monitoring of secondary cation complexation.

Cyclic voltammetry of $[\text{RuCl}(\text{PPh}_3)([\text{15}] \text{aneS}_2\text{O}_3)_2]\text{PF}_6$ under the same conditions shows a reversible $\text{Ru}^{\text{II}}-\text{Ru}^{\text{III}}$ redox couple at $E_{1/2} = +0.85$ V *vs.* ferrocene-ferrocenium. However, this couple is not affected by the addition of varying concentrations of, for example, sodium ions. This is not surprising since the ruthenium(II) complex is cationic and therefore will have a large repulsive term with respect to guest-cation complexation. In addition, the polyoxa chain is not probably long enough for efficient binding of a cation. Current work is therefore aimed at synthesising neutral or anionic ruthenium(II) complexes incorporating larger ring S_2O_x ($x > 4$) donor ionophores.

Conclusion

These results confirm that the mixed thia/oxa-donor macrocycle $[\text{15}] \text{aneS}_2\text{O}_3$ co-ordinates readily to a range of platinum-group metal ions to give 1:1 and 2:1 complexes. In each case binding is through the thioether S-donors, leaving the O-donors non-interacting and directed away from the metal. Most importantly, by introducing a bulky ligand, PPh_3 , into the co-ordination sphere of the metal ion in $[\text{RuCl}(\text{PPh}_3)([\text{15}] \text{aneS}_2\text{O}_3)_2]^+$, the conformation of the co-ordinated ionophore can be altered and, in principle, controlled and tuned. Thus, introduction of larger S_2O_n -donor ionophores and bulkier phosphine ligands would be expected to lead to better cavity definition. The presence of Cl^- or a related anion within the cavity might be an advantage under certain circumstances: if a cavity can be generated that is large enough to accommodate both Cl^- and guest cation, the attraction between the latter moieties might assist host-guest complexation.

Experimental

Infrared spectra were measured as KBr and CsI discs using a Perkin-Elmer 598 spectrometer over the range 200–4 000 cm^{-1} . U.v.-visible spectra were measured in quartz cells using Perkin-Elmer Lambda 9 and Pye Unicam SP8-400 spectrophotometers. Microanalyses were performed by the Edinburgh University Chemistry Department microanalytical service. Electrochemical measurements were performed on a Bruker E310 Universal Modular Polarograph. All readings were taken using a three-electrode potentiostatic system in acetonitrile containing 0.1 mol dm^{-3} $\text{NBu}^n_4\text{PF}_6$ or $\text{NBu}^n_4\text{BF}_4$ as supporting electrolyte. Cyclic voltammetric measurements were carried out using a double platinum electrode and a Ag-AgCl reference electrode. All potentials are quoted *versus* ferrocene-ferrocenium. Mass spectra were run by electron impact on a Kratos MS 902 and by fast-atom bombardment on a Kratos MS 50TC spectrometer. Proton and ^{13}C DEPT n.m.r. spectra were obtained on Bruker WP80 and WP200 instruments.

The ligand $[\text{15}] \text{aneS}_2\text{O}_3$ was prepared by the method of Bradshaw *et al.*¹¹

Synthesis.— $[\text{PdCl}_2([\text{15}] \text{aneS}_2\text{O}_3)]$. Treatment of PdCl_2 (40 mg, 0.226 mmol) with $[\text{15}] \text{aneS}_2\text{O}_3$ (57 mg, 0.226 mmol) in refluxing $\text{MeOH}-\text{H}_2\text{O}$ (35 cm^3 , 1:1 v/v) for 2 h under N_2 afforded a bright yellow solution. Removal of the solvent *in vacuo* yielded an orange residue which was recrystallised from EtOH and dried *in vacuo* (yield: 97 mg, 83%) (Found: C, 27.7; H, 4.7; Cl, 16.3. Calc. for $\text{C}_{10}\text{H}_{20}\text{Cl}_2\text{O}_3\text{PdS}_2$: C, 28.0; H, 4.7; Cl, 16.5%). Fast-atom bombardment mass spectrum [3-nitrobenzyl alcohol (noba)]: m/z 357; calc. for $[\text{106} \text{Pd}([\text{15}] \text{aneS}_2\text{O}_3)]^+$ 358. N.m.r. (CD_3CN , 298 K): ^1H (200.13 MHz), δ 2.28–4.18 (m, CH_2 , 20 H); ^{13}C (50.32 MHz), δ 71.07, 70.33, 69.38 (OCH_2), 37.64, and 35.73 p.p.m. (SCH_2). U.v.-visible spectrum (MeCN):

$\lambda_{\text{max.}} = 394$ nm ($\epsilon_{\text{max.}} 975 \text{ dm}^3 \text{ mol}^{-1} \text{ cm}^{-1}$), 262 (8 820). Infrared spectrum (KBr disc): 3 000w, 2 920m, 2 860m, 1 480w, 1 460m, 1 440w, 1 385m, 1 360m, 1 350w, 1 315m, 1 290w, 1 260w, 1 250m, 1 195w, 1 130m, 1 105vs, 1 080m, 1 060w, 1 040w, 1 020w, 990m, 940w, 910m, 900m, 870w, 840m, 820m, 790w, 780w, 615w, 560w, 520w, 360w, 340m, 320m, and 300 cm^{-1} .

$[\text{PtCl}_2([\text{15}] \text{aneS}_2\text{O}_3)]$. Method as above but using PtCl_2 (29 mg, 0.113 mmol) and $[\text{15}] \text{aneS}_2\text{O}_3$ (30 mg, 0.113 mmol). The product was isolated as a yellow solid (yield: 33 mg, 56%) (Found: C, 22.8; H, 3.80; Cl, 14.1; S, 11.9. Calc. for $\text{C}_{10}\text{H}_{20}\text{Cl}_2\text{O}_3\text{PtS}_2$: C, 23.2; H, 3.90; Cl, 13.7, S, 12.4%). Fast-atom bombardment mass spectrum (noba): m/z 483 and 447; calc. for $[\text{195} \text{Pt}^3\text{Cl}([\text{15}] \text{aneS}_2\text{O}_3)]^+$ 482, $[\text{195} \text{Pt}([\text{15}] \text{aneS}_2\text{O}_3)]^+$ 447. N.m.r. (CD_3NO_2 , 298 K): ^1H (200.13 MHz), δ 2.83–4.30 (m, CH_2 , 20 H); ^{13}C (50.32 MHz), δ 70.70, 70.59, 69.60 (OCH_2), 37.85, and 35.86 p.p.m. (SCH_2). U.v.-visible spectrum (MeCN): $\lambda_{\text{max.}} = 310$ nm ($\epsilon_{\text{max.}} 778 \text{ dm}^3 \text{ mol}^{-1} \text{ cm}^{-1}$), 204 (10 780). Infrared spectrum (KBr disc): 3 000w, 2 980w, 2 920m, 2 860m, 1 480w, 1 460m, 1 440m, 1 385vs, 1 360m, 1 350w, 1 310m, 1 290w, 1 245m, 1 190m, 1 130vs, 1 105vs, 1 080vs, 1 040m, 1 020vs, 985m, 970m, 940m, 910m, 900m, 870w, 840m, 820m, 790w, 655w, 615w, 560w, 520m, 490w, 480w, 450w, 440w, 380w, 360w, 330m, and 310 cm^{-1} .

$[\text{Pd}([\text{15}] \text{aneS}_2\text{O}_3)_2][\text{PF}_6]_2$. Palladium dichloride (30 mg, 0.169 mmol) was added to a solution of $[\text{15}] \text{aneS}_2\text{O}_3$ (86 mg, 0.338 mmol) in $\text{MeOH}-\text{H}_2\text{O}$ (30 cm^3 , 1:1 v/v). The reaction mixture was refluxed for 2 h under N_2 to yield a bright yellow solution. Addition of an excess of NH_4PF_6 gave a yellow precipitate which was collected, recrystallised from MeNO_2 and dried *in vacuo* (yield: 110 mg, 73%) (Found: C, 26.4; H, 4.45; S, 15.2. Calc. for $\text{C}_{20}\text{H}_{40}\text{F}_{12}\text{O}_6\text{P}_2\text{PdS}_4$: C, 26.7; H, 4.45; S, 14.3%). Fast-atom bombardment mass spectrum (noba): m/z 610 and 358; calc. for $[\text{106} \text{Pd}([\text{15}] \text{aneS}_2\text{O}_3)_2]^+$ 610, $[\text{106} \text{Pd}([\text{15}] \text{aneS}_2\text{O}_3)]^+$ 358. N.m.r. ^1H [200.13 MHz, (CD_3)₂CO, 298 K], δ 3.96, 3.62, and 3.35 (m, CH_2 , 40 H); ^{13}C (50.32 MHz, CD_3CN , 298 K), δ 69.99, 68.84, 68.15 (OCH_2), and 37.11 p.p.m. (SCH_2), two overlapping resonances). U.v.-visible spectrum (MeCN): $\lambda_{\text{max.}} = 305$ nm ($\epsilon_{\text{max.}} 32 790 \text{ dm}^3 \text{ mol}^{-1} \text{ cm}^{-1}$). Infrared spectrum (KBr disc): 2 980w, 2 920m, 2 860m, 1 470m, 1 455m, 1 395m, 1 365m, 1 300m, 1 260w, 1 200w, 1 180w, 1 120vs, 1 090vs, 1 040m, 1 020w, 965w, 930m, 840vs, 780m, 740w, 555vs, and 480 cm^{-1} .

$[\text{Pt}([\text{15}] \text{aneS}_2\text{O}_3)_2][\text{PF}_6]_2$. Method as above but using PtCl_2 (40 mg, 0.150 mmol) and $[\text{15}] \text{aneS}_2\text{O}_3$ (76 mg, 0.301 mmol). The product was isolated as a cream coloured solid (yield: 74 mg, 50%) (Found: C, 24.2; H, 4.10; S, 13.4. Calc. for $\text{C}_{20}\text{H}_{40}\text{F}_{12}\text{O}_6\text{P}_2\text{PtS}_4$: C, 24.3; H, 4.05; S, 13.0%). Fast-atom bombardment mass spectrum (noba): m/z 699 and 446; calc. for $[\text{195} \text{Pt}([\text{15}] \text{aneS}_2\text{O}_3)_2]^+$ 699, $[\text{195} \text{Pt}([\text{15}] \text{aneS}_2\text{O}_3)]^+$ 447. N.m.r. (CD_3CN , 298 K): ^1H (200.13 MHz), δ 3.2–4.2 (m, CH_2 , 40 H); ^{13}C (50.32 MHz), δ 70.17, 69.33, 69.00 (OCH_2), 37.57, and 36.86 p.p.m. (SCH_2). U.v.-visible spectrum (MeCN): $\lambda_{\text{max.}} = 326$ nm ($\epsilon_{\text{max.}} 158 \text{ dm}^3 \text{ mol}^{-1} \text{ cm}^{-1}$), 249 (9 150). Infrared spectrum (KBr disc): 3 020w, 2 920m, 2 860w, 1 475m, 1 455m, 1 415m, 1 400m, 1 365m, 1 350w, 1 300m, 1 260w, 1 245w, 1 195m, 1 180w, 1 120vs, 1 090m, 1 065w, 1 040m, 1 020w, 965w, 930m, 840vs, 775m, 740w, 660w, 610w, 555vs, and 480 cm^{-1} .

$[\text{RhCl}_2([\text{15}] \text{aneS}_2\text{O}_3)_2]\text{PF}_6$. The compound $\text{RhCl}_3 \cdot 3\text{H}_2\text{O}$ (30 mg, 0.114 mmol) was added to a refluxing solution of $[\text{15}] \text{aneS}_2\text{O}_3$ (57 mg, 0.228 mmol) in MeOH (30 cm^3). The reaction mixture was refluxed for 4 h under N_2 to afford a bright yellow solution. Addition of an excess of NH_4PF_6 gave an orange precipitate which was collected, recrystallised from MeNO_2 and dried *in vacuo* (yield: 85 mg, 91%) (Found: C, 28.5; H, 4.85; Cl, 8.75; S, 16.6. Calc. for $\text{C}_{20}\text{H}_{40}\text{Cl}_2\text{F}_6\text{O}_6\text{PRhS}_4$: C, 29.2; H, 4.90; Cl, 8.60; S, 15.6%). Fast-atom bombardment mass spectrum (noba): m/z 677 and 642; calc. for $[\text{103} \text{Rh}^3\text{Cl}_2([\text{15}] \text{aneS}_2\text{O}_3)_2]^+$

Table 1. Bond lengths (Å), angles and torsion angles (°) for [Pd([15]aneS₂O₃)₂][PF₆]₂ with estimated standard deviations (e.s.d.s) in parentheses

Pd-S(1)	2.314 9(10)	O(7)-C(8)	1.417(6)
Pd-S(4)	2.301 7(10)	C(8)-C(9)	1.492(7)
S(1)-C(2)	1.818(4)	C(9)-O(10)	1.403(6)
S(1)-C(15)	1.819(5)	O(10)-C(11)	1.418(6)
C(2)-C(3)	1.507(5)	C(11)-C(12)	1.478(7)
C(3)-S(4)	1.813(4)	C(12)-O(13)	1.441(6)
S(4)-C(5)	1.821(4)	O(13)-C(14)	1.413(5)
C(5)-C(6)	1.502(7)	C(14)-C(15)	1.522(6)
C(6)-O(7)	1.406(6)		
S(1)-Pd-S(4)	89.78(4)	C(5)-C(6)-O(7)	111.1(4)
Pd-S(1)-C(2)	101.99(13)	C(6)-O(7)-C(8)	116.3(4)
Pd-S(1)-C(15)	108.40(15)	O(7)-C(8)-C(9)	109.7(4)
C(2)-S(1)-C(15)	102.48(19)	C(8)-C(9)-O(10)	110.1(4)
S(1)-C(2)-C(3)	108.7(3)	C(9)-O(10)-C(11)	113.3(3)
C(2)-C(3)-S(4)	112.3(3)	O(10)-C(11)-C(12)	109.6(4)
Pd-S(4)-C(3)	100.01(13)	C(11)-C(12)-O(13)	109.8(4)
Pd-S(4)-C(5)	103.16(14)	C(12)-O(13)-C(14)	114.8(3)
C(3)-S(4)-C(5)	104.81(19)	O(13)-C(14)-C(15)	112.9(4)
S(4)-C(5)-C(6)	110.9(3)	S(1)-C(15)-C(14)	111.4(3)
C(15)-S(1)-C(2)-C(3)	-153.4(3)		
C(2)-S(1)-C(15)-C(14)	-71.0(3)		
S(1)-C(2)-C(3)-S(4)	60.1(3)		
C(2)-C(3)-S(4)-C(5)	61.1(3)		
C(3)-S(4)-C(5)-C(6)	61.0(3)		
S(4)-C(5)-C(6)-O(7)	-76.7(4)		
C(5)-C(6)-O(7)-C(8)	-109.8(4)		
C(6)-O(7)-C(8)-C(9)	152.3(4)		
O(7)-C(8)-C(9)-O(10)	-72.9(5)		
C(8)-C(9)-O(10)-C(11)	-171.1(4)		
C(9)-O(10)-C(11)-C(12)	-171.7(4)		
O(10)-C(11)-C(12)-O(13)	77.4(5)		
C(11)-C(12)-O(13)-C(14)	-156.3(4)		
C(12)-O(13)-C(14)-C(15)	87.3(4)		
O(13)-C(14)-C(15)-S(1)	69.5(4)		

aneS₂O₃)₂)⁺ 677, [¹⁰³Rh³⁵Cl([15]aneS₂O₃)₂)⁺ 642. N.m.r. (CD₃CN, 298 K): ¹H (200.13 MHz), δ 2.67–4.30 (m, CH₂, 40 H); ¹³C (50.32 MHz), δ 69.55, 69.40, 67.85 (OCH₂), 36.59, and 33.53 p.p.m. (SCH₂). U.v.-visible spectrum (MeCN): λ_{max} = 435 nm (ε_{max}, 132 dm³ mol⁻¹ cm⁻¹), 283 (32 970). Infrared spectrum (KBr disc): 3 000w, 2 900m, 2 860m, 1 535m, 1 460m, 1 400m, 1 360m, 1 345w, 1 290vs, 1 240m, 1 210w, 1 195m, 1 170m, 1 140vs, 1 100vs, 1 080vs, 1 050m, 1 020m, 1 005w, 935m, 920m, 895m, 875m, 840vs, 775m, 665m, 555vs, 485m, 470m, 450w, and 350m cm⁻¹.

[IrCl₂([15]aneS₂O₃)₂][PF₆]. Method as above but using IrCl₃·3H₂O (75 mg, 0.213 mmol) and [15]aneS₂O₃ (108 mg, 0.425 mmol). The product was isolated as a pale yellow solid which was collected, recrystallised from MeNO₂, and dried *in vacuo* (yield: 55 mg, 28%) (Found: C, 26.0; H, 4.25; S, 13.2. Calc. for C₂₀H₄₀Cl₂F₆IrO₆PS₄: C, 26.3; H, 4.40; S, 14.0%). Fast-atom bombardment mass spectrum (noba): *m/z* 767, 733, 696, and 444; calc. for [¹⁹³Ir³⁵Cl₂([15]aneS₂O₃)₂)⁺ 767, [¹⁹³Ir³⁵Cl([15]aneS₂O₃)₂)⁺ 732, [¹⁹³Ir([15]aneS₂O₃)₂)⁺ 697, [¹⁹³Ir([15]aneS₂O₃)⁺ 445. N.m.r. (CD₃CN, 298 K): ¹H (80.13 MHz), δ 3.3–4.2 (m, CH₂, 40 H); ¹³C (50.32 MHz), δ 69.68, 69.54, 67.67 (OCH₂), 35.76, and 32.60 p.p.m. (SCH₂). U.v.-visible spectrum (MeCN): λ_{max} = 236 nm (ε_{max} = 24 860 dm³ mol⁻¹ cm⁻¹). Infrared spectrum (KBr disc): 3 000w, 2 900m, 2 860m, 1 460m, 1 405m, 1 360m, 1 350w, 1 290m, 1 240w, 1 205w, 1 135m, 1 110m, 1 100m, 1 070m, 1 050w, 1 015w, 1 000w, 935m, 895w, 840vs, 740w, 555vs, 485w, 470w, 330m, 315m, and 300m cm⁻¹.

Table 2. Fractional atomic co-ordinates with e.s.d.s for [Pd([15]aneS₂O₃)₂][PF₆]₂

Atom	x	y	z
Pd	0.5	0.5	0.5
S(1)	0.696 97(9)	0.556 02(7)	0.466 23(9)
C(2)	0.805 0(4)	0.452 7(3)	0.504 2(3)
C(3)	0.780 1(4)	0.407 0(3)	0.613 7(4)
S(4)	0.609 73(9)	0.367 75(7)	0.592 83(9)
C(5)	0.585 5(4)	0.279 7(3)	0.474 6(4)
C(6)	0.678 9(5)	0.197 0(3)	0.509 6(5)
O(7)	0.807 8(3)	0.221 13(21)	0.502 0(3)
C(8)	0.853 1(5)	0.177 1(3)	0.409 8(5)
C(9)	0.952 7(5)	0.239 9(3)	0.374 4(4)
O(10)	0.889 2(3)	0.319 11(22)	0.311 2(3)
C(11)	0.974 1(4)	0.374 5(3)	0.259 2(4)
C(12)	0.905 5(5)	0.463 4(4)	0.209 9(4)
O(13)	0.906 6(3)	0.530 39(23)	0.303 8(3)
C(14)	0.804 6(4)	0.599 5(3)	0.278 2(4)
C(15)	0.677 2(4)	0.565 7(3)	0.307 5(4)
P(1)	0.336 07(12)	0.385 46(8)	0.136 51(11)
F(1)	0.484 6(4)	0.355 4(4)	0.188 4(4)
F(2)	0.369 8(6)	0.485 4(3)	0.198 5(5)
F(3)	0.374 1(4)	0.424 4(3)	0.024 8(3)
F(4)	0.189 5(4)	0.419 6(4)	0.087 0(4)
F(5)	0.306 4(6)	0.288 5(3)	0.075 7(6)
F(6)	0.300 5(5)	0.348 7(4)	0.251 1(4)

[RuCl₂(PPh₃)([15]aneS₂O₃)₂][PF₆]. Treatment of [RuCl₂(PPh₃)₃] (100 mg, 0.104 mmol) with [15]aneS₂O₃ (53 mg, 0.208 mmol) in refluxing MeOH (30 cm³) for 2 h under N₂ affords a yellow solution. Addition of an excess of NH₄PF₆ gave a yellow product which was collected and recrystallised from CH₂Cl₂ (yield: 100 mg, 92%) (Found: C, 44.1; H, 5.35. Calc. for C₃₈H₅₅ClF₆O₆P₂RuS₄: C, 44.7; H, 5.45%). Fast-atom bombardment mass spectrum (noba): *m/z* 1 046, 904, 650, and 640; calc. for [¹⁰²Ru³⁵Cl(PPh₃)([15]aneS₂O₃)₂(PF₆)⁺ 1 048, [¹⁰²Ru³⁵Cl(PPh₃)([15]aneS₂O₃)₂)⁺ 903, [¹⁰²Ru³⁵Cl(PPh₃)([15]aneS₂O₃)⁺ 651, [¹⁰²Ru³⁵Cl([15]aneS₂O₃)₂)⁺ 641. N.m.r.: ¹H (80.13 MHz, CD₃NO₂, 298 K), δ 7.3–8.0 (m, Ph, 15 H) and 2.0–4.3 (m, CH₂, 40 H); ¹³C [50.32 MHz, (CD₃)₂CO, 298 K], δ 134.01 (d), 131.06 (d), 129.67 (d), 127.29 (d) (C of Ph rings), 69.36, 68.54 (two overlapping) (OCH₂), 32.04, and 30.56 p.p.m. (SCH₂). Infrared spectrum (KBr disc): 3 040w, 2 920m, 2 860m, 1 585w, 1 570w, 1 480m, 1 455w, 1 430m, 1 410m, 1 360m, 1 290m, 1 190w, 1 130m, 1 110m, 1 090m, 1 000w, 840vs, 750m, 700vs, 555vs, 530vs, 515m, 505w, and 465w cm⁻¹.

X-Ray Structure Determination of [Pd([15]aneS₂O₃)₂][PF₆]₂.—An orange plate (1.0 × 0.10 × 0.75 mm) suitable for X-ray analysis was obtained by vapour-diffusion of diethyl ether into a solution of the complex in MeCN.

Crystal data. C₂₀H₄₀O₆PdS₄·2PF₆⁻, *M* = 901.0, monoclinic, space group *P*₂₁/*c* with *a* = 10.394(4), *b* = 14.003(4), *c* = 11.675(5) Å, β = 104.22(3)°, *U* = 1 647 Å³ [from 2θ values of 25 reflections measured at ±ω (36 ≤ 2θ ≤ 38°, λ = 0.710 73 Å, *T* = 298 K)], *D*_c = 1.816 g cm⁻³, *Z* = 2, *F*(000) = 912, μ(Mo-*K*_α) = 9.95 cm⁻¹.

Data collection and processing. Stoë STADI-4 four-circle diffractometer, graphite monochromated Mo-*K*_α radiation, ω–2θ scans, 2 808 unique reflections measured (2θ_{max} = 45°, *h* –12 to 12, *k* 0–16, *l* 0–12), initial absorption corrections (min. 0.985, max. 1.015) made using ψ scans, giving 2 402 with *F* ≥ 6σ(*F*). No significant crystal decay or movement was observed.

Structure analysis and refinement. Intensity statistics strongly implied the location of the Pd atom at (½, ½, ½). Using this

Table 3. Bond lengths (Å), angles and torsion angles (°) with e.s.d.s for [RuCl(PPh₃)([15]aneS₂O₃)₂]PF₆·H₂O

Ru-S(1)	2.394(3)	S(4)-C(5)	1.818(12)	C(14)-C(15)	1.522(19)	C(9')-O(10')	1.395(22)
Ru-S(4)	2.395(3)	C(5)-C(6)	1.531(17)	S(1')-C(2')	1.835(12)	O(10')-C(11')	1.391(20)
Ru-S(1')	2.390(3)	C(6)-O(7)	1.398(14)	S(1')-C(15')	1.809(13)	C(11')-C(12')	1.451(22)
Ru-S(4')	2.405(3)	O(7)-C(8)	1.405(16)	C(2')-C(3')	1.506(16)	C(12')-O(13')	1.427(18)
Ru-P(1)	2.319(3)	C(8)-C(9)	1.464(21)	C(3')-S(4')	1.806(12)	O(13')-C(14')	1.409(16)
Ru-Cl(1)	2.458(3)	C(9)-O(10)	1.407(18)	S(4')-C(5')	1.824(13)	C(14')-C(15')	1.519(19)
S(1)-C(2)	1.840(12)	O(10)-C(11)	1.333(23)	C(5')-C(6')	1.508(19)	P(1)-C(1R)	1.849(8)
S(1)-C(15)	1.845(14)	C(11)-C(12)	1.49(3)	C(6')-O(7')	1.386(17)	P(1)-C(7R)	1.852(7)
C(2)-C(3)	1.494(16)	C(12)-O(13)	1.356(22)	O(7')-C(8')	1.342(22)	P(1)-C(13R)	1.849(8)
C(3)-S(4)	1.787(12)	O(13)-C(14)	1.401(18)	C(8')-C(9')	1.48(3)		
S(1)-Ru-S(4)	84.98(10)	S(1)-C(2)-C(3)	108.6(8)	S(1)-C(15)-C(14)	114.6(9)	C(12')-O(13')-C(14')	113.5(10)
S(1)-Ru-S(1')	101.67(11)	C(2)-C(3)-S(4)	111.9(8)	Ru-S(1')-C(2')	101.8(4)	O(13')-C(14')-C(15')	116.3(11)
S(1)-Ru-S(4')	173.26(11)	Ru-S(4)-C(3)	104.4(4)	Ru-S(1')-C(15')	113.8(4)	S(1')-C(15')-C(14')	113.9(9)
S(1)-Ru-P(1)	88.77(11)	Ru-S(4)-C(5)	111.6(4)	C(2')-S(1')-C(15')	99.9(6)	Ru-P(1)-C(1R)	118.5(3)
S(1)-Ru-Cl(1)	88.23(11)	C(3)-S(4)-C(5)	104.1(5)	S(1')-C(2')-C(3')	109.9(8)	Ru-P(1)-C(7R)	114.83(25)
S(4)-Ru-S(1')	173.21(11)	S(4)-C(5)-C(6)	115.3(8)	C(2')-C(3')-S(4')	110.5(8)	Ru-P(1)-C(13R)	115.1(3)
S(4)-Ru-S(4')	88.29(10)	C(5)-C(6)-O(7)	114.0(10)	Ru-S(4')-C(3')	104.8(4)	C(1R)-P(1)-C(7R)	101.1(3)
S(4)-Ru-P(1)	91.59(10)	C(6)-O(7)-C(8)	113.9(9)	Ru-S(4')-C(5')	110.8(4)	C(1R)-P(1)-C(13R)	99.5(4)
S(4)-Ru-Cl(1)	92.01(10)	O(7)-C(8)-C(9)	111.2(11)	C(3')-S(4')-C(5')	104.2(6)	C(7R)-P(1)-C(13R)	105.6(3)
S(1')-Ru-S(4)	85.07(11)	C(8)-C(9)-O(10)	108.7(12)	S(4')-C(5')-C(6')	115.5(9)	P(1)-C(1R)-C(2R)	117.8(6)
S(1')-Ru-P(1)	87.25(11)	C(9)-O(10)-C(11)	114.3(13)	C(5')-C(6')-O(7')	115.2(11)	P(1)-C(1R)-C(6R)	122.2(6)
S(1')-Ru-Cl(1)	89.56(11)	O(10)-C(11)-C(12)	110.1(16)	C(6')-O(7')-C(8')	119.4(13)	P(1)-C(7R)-C(8R)	119.7(5)
S(4')-Ru-P(1)	91.76(11)	C(11)-C(12)-O(13)	114.3(16)	O(7')-C(8')-C(9')	116.5(16)	P(1)-C(7R)-C(12R)	120.1(5)
S(4')-Ru-Cl(1)	91.67(10)	C(12)-O(13)-C(14)	117.0(13)	C(8')-C(9')-O(10')	113.3(15)	P(1)-C(13R)-C(14R)	120.8(6)
P(1)-Ru-Cl(1)	175.10(11)	O(13)-C(14)-C(15)	114.6(11)	C(9')-O(10')-C(11')	114.9(13)	P(1)-C(13R)-C(18R)	118.8(6)
Ru-S(1)-C(2)	101.4(4)			O(10')-C(11')-C(12')	104.9(13)		
Ru-S(1)-C(15)	113.4(4)			C(11')-C(12')-O(13')	112.4(13)		
C(2)-S(1)-C(15)	101.0(6)						
C(15)-S(1)-C(2)-C(3)	-167.3(8)	C(2')-C(3')-S(4')-C(5')	-79.0(9)	C(13R)-P(1)-C(7R)-C(8R)	61.7(6)		
C(2)-S(1)-C(15)-C(14)	-54.6(11)	C(3')-S(4')-C(5')-C(6')	-38.7(11)	C(13R)-P(1)-C(7R)-C(12R)	-123.4(6)		
S(1)-C(2)-C(3)-S(4)	60.2(9)	S(4')-C(5')-C(6')-O(7')	78.8(13)	C(1R)-P(1)-C(13R)-C(14R)	-155.7(7)		
C(2)-C(3)-S(4)-C(5)	79.5(9)	C(5')-C(6')-O(7')-C(8')	94.6(16)	C(1R)-P(1)-C(13R)-C(18R)	31.5(7)		
C(3)-S(4)-C(5)-C(6)	42.5(10)	C(6')-O(7')-C(8')-C(9')	-163.1(14)	C(7R)-P(1)-C(13R)-C(14R)	-51.2(7)		
S(4)-C(5)-C(6)-O(7)	-84.4(11)	O(7')-C(8')-C(9')-O(10')	59.8(21)	C(7R)-P(1)-C(13R)-C(18R)	136.0(6)		
C(5)-C(6)-O(7)-C(8)	-81.0(12)	C(8')-C(9')-O(10')-C(11')	176.4(14)	C(3R)-C(2R)-C(1R)-P(1)	-179.2(6)		
C(6)-O(7)-C(8)-C(9)	164.8(11)	C(9')-O(10')-C(11')-C(12')	178.3(13)	C(5R)-C(6R)-C(1R)-P(1)	179.2(6)		
O(7)-C(8)-C(9)-O(10)	-73.4(14)	O(10')-C(11')-C(12')-O(13')	-72.3(15)	C(9R)-C(8R)-C(7R)-P(1)	174.9(5)		
C(8)-C(9)-O(10)-C(11)	-174.8(14)	C(11')-C(12')-O(13')-C(14')	161.7(12)	C(9R)-C(8R)-C(7R)-C(12R)	-0.1(10)		
C(9)-O(10)-C(11)-C(12)	-176.8(14)	C(12')-O(13')-C(14')-C(15')	-75.8(14)	C(8R)-C(9R)-C(10R)-C(11R)	0.0(10)		
O(10)-C(11)-C(12)-O(13)	69.6(21)	O(13')-C(14')-C(15')-S(1')	-75.3(13)	C(9R)-C(10R)-C(11R)-C(12R)	0.0(10)		
C(11)-C(12)-O(13)-C(14)	-161.4(15)	C(7R)-P(1)-C(1R)-C(2R)	-53.7(7)	C(10R)-C(11R)-C(12R)-C(7R)	-0.1(10)		
C(12)-O(13)-C(14)-C(15)	77.5(17)	C(7R)-P(1)-C(1R)-C(6R)	127.1(7)	C(11R)-C(12R)-C(7R)-P(1)	-174.9(5)		
O(13)-C(14)-C(15)-S(1)	73.1(13)	C(13R)-P(1)-C(1R)-C(2R)	54.5(7)	C(15R)-C(14R)-C(13R)-P(1)	-172.7(6)		
C(15)-S(1)-C(2)-C(3)	167.0(8)	C(13R)-P(1)-C(1R)-C(6R)	-124.8(7)	C(17R)-C(18R)-C(13R)-P(1)	172.9(6)		
C(2')-S(1')-C(15')-C(14')	60.9(10)	C(1R)-P(1)-C(7R)-C(8R)	165.0(6)				
S(1')-C(2')-C(3')-S(4')	-59.4(9)	C(1R)-P(1)-C(7R)-C(12R)	-20.1(6)				

information, DIRDIF²⁴ located all other non-H atoms. At isotropic convergence, final corrections (min. 0.875, max. 1.290) for absorption were made using DIFABS.²⁵ Anisotropic thermal parameters were refined for all non-H atoms, H atoms were included in fixed, calculated positions.²⁶ The weighting scheme $w^{-1} = \sigma^2(F) + 0.000 187F^2$ gave satisfactory agreement analyses. At convergence, R , R' = 0.0394, 0.0537 respectively for 205 parameters, S = 1.195. The maximum and minimum residues in the final ΔF syntheses were +0.67 and -0.51 e Å⁻³ respectively. Bond lengths, angles and torsion angles are given in Table 1 and fractional atomic co-ordinates in Table 2.

X-Ray Structure Determination of [RuCl(PPh₃)([15]aneS₂O₃)₂]PF₆·H₂O.—A yellow lath (0.08 × 0.23 × 0.38 mm) suitable for X-ray analysis was obtained by recrystallisation of the complex from CH₂Cl₂-EtOH.

Crystal data. C₃₈H₅₅ClO₆PRuS₄·PF₆·H₂O, M = 1 066.5, orthorhombic, space group $Pbcn$ with a = 19.252 6(14), b = 25.968(3), c = 18.903 3(23) Å, U = 9 451 Å³, D_c = 1.499 g cm⁻³, Z = 8; $F(000)$ = 4 400, $\mu(\text{Mo-K}\alpha)$ = 6.84 cm⁻¹.

Data collection and processing. STADI-4 diffractometer, graphite-monochromated Mo-K α radiation, ω —2 θ scans, 7 634 reflections measured ($2\theta_{\text{max}}$ = 45°, h 0—20, k 0—27, l 0—20) giving 3 127 with $F \geq 6\sigma(F)$. No significant crystal decay, no absorption correction.

Structure analysis and refinement. The Ru atom was located by a Patterson synthesis. The structure was developed by iterative rounds of least-squares refinement and difference Fourier synthesis.²⁴ Two half-occupied, mutually incompatible water molecules were found to be H-bonded to each complex cation. The phenyl rings of the PPh₃ ligand were refined as idealised hexagons. Anisotropic thermal parameters were refined for Ru, Cl, P, S, F, and all fully occupied O atoms. H atoms were included in fixed, calculated positions.²⁴ The weighting scheme $w^{-1} = \sigma^2(F) + 0.000 793F^2$ gave satisfactory agreement analyses. At convergence, R , R' = 0.0603, 0.0774 respectively for 305 parameters, S = 1.111. The maximum and minimum residues in the final ΔF syntheses were +0.60 and -0.46 e Å⁻³ respectively. Illustrations were prepared using ORTEP,²⁷ molecular geometry calculations utilised CALC,²⁸

Table 4. Fractional atomic co-ordinates with e.s.d.s for [RuCl(PPh₃)([15]aneS₂O₃)₂]PF₆·H₂O*

Atom	x	y	z	Atom	x	y	z
Ru	0.255 25(4)	0.378 53(3)	0.485 23(5)	C(2')	0.394 7(6)	0.342 2(4)	0.397 1(7)
S(1)	0.161 46(15)	0.330 80(12)	0.536 30(18)	C(3')	0.416 2(5)	0.395 1(4)	0.421 0(6)
S(4)	0.182 31(14)	0.452 06(11)	0.503 44(15)	C(5')	0.315 5(6)	0.455 5(5)	0.346 5(7)
O(7)	0.019 7(4)	0.474 4(3)	0.427 3(4)	C(6')	0.374 6(7)	0.467 6(5)	0.296 9(7)
O(10)	-0.014 1(5)	0.370 6(4)	0.383 5(6)	C(8')	0.386 5(10)	0.408 5(7)	0.203 2(10)
O(13)	0.007 1(5)	0.285 0(4)	0.478 2(6)	C(9')	0.407 8(9)	0.355 7(7)	0.183 3(10)
S(1')	0.338 84(16)	0.312 23(11)	0.464 11(17)	C(11')	0.398 4(8)	0.267 6(6)	0.210 0(9)
S(4')	0.340 90(15)	0.435 27(11)	0.435 21(17)	C(12')	0.365 9(8)	0.235 8(6)	0.263 8(8)
O(7')	0.407 0(6)	0.425 1(4)	0.267 1(6)	C(14')	0.361 0(7)	0.221 7(5)	0.387 7(8)
O(10')	0.382 9(7)	0.318 0(4)	0.229 4(6)	C(15')	0.305 3(6)	0.258 5(5)	0.413 6(7)
O(13')	0.401 4(4)	0.238 5(3)	0.330 0(5)	C(2R)	0.339 5(4)	0.334 1(3)	0.720 2(4)
P(1)	0.303 01(15)	0.386 77(11)	0.597 27(16)	C(3R)	0.347 2(4)	0.291 2(3)	0.764 0(4)
Cl(1)	0.204 12(16)	0.361 83(11)	0.368 31(16)	C(4R)	0.325 9(4)	0.242 8(3)	0.740 6(4)
P(2)	0.271 05(24)	0.385 31(15)	-0.008 5(3)	C(5R)	0.297 0(4)	0.237 2(3)	0.673 3(4)
F(1)	0.247 6(9)	0.332 7(4)	0.019 1(7)	C(6R)	0.289 4(4)	0.280 1(3)	0.629 5(4)
F(2)	0.293 0(7)	0.437 7(5)	-0.037 9(10)	C(1R)	0.310 6(4)	0.328 5(3)	0.653 0(4)
F(3)	0.254 2(10)	0.406 1(7)	0.062 3(10)	C(8R)	0.252 7(4)	0.483 20(24)	0.642 2(3)
F(4)	0.293 2(9)	0.360 7(7)	-0.076 0(8)	C(9R)	0.212 3(4)	0.515 88(24)	0.684 0(3)
F(5)	0.345 2(7)	0.379 4(8)	0.015 1(9)	C(10R)	0.174 6(4)	0.496 00(24)	0.740 8(3)
F(6)	0.198 5(7)	0.395 0(7)	-0.032 1(13)	C(11R)	0.177 2(4)	0.443 45(24)	0.755 8(3)
C(2)	0.088 1(5)	0.375 1(4)	0.522 4(6)	C(12R)	0.217 6(4)	0.410 77(24)	0.714 1(3)
C(3)	0.108 2(6)	0.427 1(4)	0.548 9(7)	C(7R)	0.255 3(4)	0.430 64(24)	0.657 3(3)
C(5)	0.147 3(6)	0.476 2(4)	0.420 5(6)	C(14R)	0.410 9(4)	0.460 4(3)	0.587 7(5)
C(6)	0.078 7(6)	0.505 8(5)	0.426 7(7)	C(15R)	0.480 2(4)	0.475 3(3)	0.581 4(5)
C(8)	-0.001 7(8)	0.458 3(5)	0.359 8(8)	C(16R)	0.532 9(4)	0.438 7(3)	0.586 6(5)
C(9)	-0.050 8(7)	0.415 4(5)	0.364 4(8)	C(17R)	0.516 3(4)	0.387 1(3)	0.598 2(5)
C(11)	-0.052 4(10)	0.327 9(8)	0.383 8(12)	C(18R)	0.447 0(4)	0.372 1(3)	0.604 5(5)
C(12)	-0.009 9(10)	0.283 3(7)	0.408 6(11)	C(13R)	0.394 3(4)	0.408 8(3)	0.599 3(5)
C(14)	0.062 6(7)	0.254 1(5)	0.500 2(8)	O(1S)	0.487 5(15)	0.123 1(10)	0.215 2(13)
C(15)	0.134 2(6)	0.275 2(5)	0.482 2(8)	O(2S)	0.473 2(17)	0.132 6(13)	0.322 9(19)

* Carbon atoms of the phenyl groups of PPh₃ are indicated by R, O atoms of the solvent water by S.

and scattering factor data were taken from ref. 29. Bond lengths, angles, and torsion angles are given in Table 3 and fractional co-ordinates are given in Table 4.

Additional material available from the Cambridge Crystallographic Data Centre comprises H-atom co-ordinates, thermal parameters, and remaining bond lengths and angles.

Acknowledgements

We thank the S.E.R.C. for support and Johnson Matthey plc for generous loans of platinum metal salts.

References

- D. E. Koshland, 'Enzymes,' 3rd edn., ed. H. U. Bergmeyer, 1970, vol. 1, p. 341; J. Rebek, *Acc. Chem. Res.*, 1984, **17**, 258.
- J. Rebek, J. E. Trend, R. V. Whattley, and S. Chakravorty, *J. Am. Chem. Soc.*, 1979, **101**, 4333; J. Rebek and L. Marshall, *ibid.*, 1983, **105**, 6668; N. A. Obaidi, P. D. Beer, J. P. Bright, C. J. Jones, J. A. McCleverty, and S. S. Salam, *J. Chem. Soc., Chem. Commun.*, 1986, 239; P. D. Beer, *ibid.*, p. 1678; J.-C. Chambron and J.-P. Sauvage, *Tetrahedron Lett.*, 1986, **27**, 865; A. Hamilton, J.-M. Lehn, and J. L. Sessler, *J. Am. Chem. Soc.*, 1986, **108**, 5158; C. J. van Staveren, D. N. Rheinhoudt, J. van Eerden, and S. Harkema, *J. Chem. Soc., Chem. Commun.*, 1987, 974.
- M. P. Andrews, C. Blackburn, J. F. McAleer, and V. D. Patel, *J. Chem. Soc., Chem. Commun.*, 1987, 1122 and refs. therein.
- P. D. Beer, H. Sikanyika, A. M. S. Slawin, and D. J. Williams, *Polyhedron*, 1989, **8**, 879; P. D. Beer, E. L. Tite, and A. Ibbotson, *J. Chem. Soc., Chem. Commun.*, 1989, 1874 and refs. therein.
- E. Fu, M. L. H. Green, V. J. Lowe, and S. R. Marder, *J. Organomet. Chem.*, 1988, **341**, C39 and refs. therein.
- M. Schröder, *Pure Appl. Chemistry*, 1988, **60**, 517; A. J. Blake and M. Schröder, *Adv. Inorg. Chem.*, 1990, **35**, 1.
- R. E. DeSimone and M. D. Glick, *J. Am. Chem. Soc.*, 1975, **97**, 942; R. E. DeSimone and T. M. Tighe, *J. Inorg. Nucl. Chem.*, 1976, **38**, 1623; N. W. Alcock, N. Herron, and P. Moore, *J. Chem. Soc., Chem. Commun.*, 1976, 886; N. W. Alcock, N. Herron, and P. Moore, *J. Chem. Soc., Dalton Trans.*, 1978, 394; D. P. Riley and J. D. Oliver, *Inorg. Chem.*, 1983, **22**, 3361; M. N. Bell, A. J. Blake, M. Schröder, and T. A. Stephenson, *J. Chem. Soc., Chem. Commun.*, 1986, 471; G. H. Robinson, H. Zhang, and J. L. Atwood, *Organometallics*, 1987, **6**, 887.
- G. H. Robinson and S. A. Sangokoya, *J. Am. Chem. Soc.*, 1988, **110**, 1494.
- R. E. DeSimone and M. D. Glick, *J. Am. Chem. Soc.*, 1976, **98**, 762; J. R. Hartman, R. E. Wolf, B. M. Foxman, and S. R. Cooper, *J. Am. Chem. Soc.*, 1983, **105**, 131; R. E. Wolf, J. R. Hartman, J. M. E. Storey, B. M. Foxman, and S. R. Cooper, *J. Am. Chem. Soc.*, 1987, **109**, 4328.
- S. G. Murray and F. R. Hartley, *Chem. Rev.*, 1981, **81**, 365.
- J. S. Bradshaw, J. Y. Hui, B. L. Haymore, J. J. Christensen, and R. M. Izatt, *J. Heterocycl. Chem.*, 1973, **10**, 1.
- J. S. Bradshaw, R. A. Reeder, M. D. Thompson, and J. J. Christensen, *J. Org. Chem.*, 1976, **41**, 134.
- J. S. Bradshaw, J. Y. Hui, Y. Chan, B. L. Haymore, R. M. Izatt, and J. J. Christensen, *J. Heterocycl. Chem.*, 1974, **11**, 45.
- N. K. Dalley, S. B. Larson, J. S. Smith, K. L. Matheson, R. M. Izatt, and J. J. Christensen, *J. Heterocycl. Chem.*, 1981, **18**, 463.
- C. J. Pedersen, *J. Am. Chem. Soc.*, 1967, **89**, 1080.
- C. J. Pedersen, *J. Am. Chem. Soc.*, 1967, **89**, 7017.
- For example see: 'Synthetic Multidentate Macrocyclic Compounds,' eds. R. M. Izatt and J. J. Christensen, Academic Press, New York, 1978; 'Coordination Chemistry of Macrocyclic Compounds,' ed. G. A. Melson, Plenum Press, New York, 1979; 'Host Guest Complex Chemistry: Macrocycles,' eds. F. Vögtle and E. Weber, Springer, Berlin, 1985; L. F. Lindoy, 'The Chemistry of Macrocyclic Ligand Complexes,' Cambridge University Press, Cambridge, 1989.
- D. J. Cram, *Angew. Chem., Int. Ed. Engl.*, 1988, **27**, 1009.
- R. M. Izatt, R. E. Terry, L. D. Hansen, A. G. Avondet, J. S. Bradshaw,

- N. K. Dalley, T. E. Jensen, and B. L. Haymore, *Inorg. Chim. Acta*, 1978, **30**, 1.
- 20 B. Metz, D. Moras, and R. Weiss, *J. Inorg. Nucl. Chem.*, 1974, **36**, 785.
- 21 A. J. Blake, R. O. Gould, A. J. Lavery, and M. Schröder, *Angew. Chem.*, 1986, **98**, 282; *Angew. Chem., Int. Ed. Engl.*, 1986, **25**, 274; A. J. Blake, R. O. Gould, A. J. Holder, T. I. Hyde, M. O. Odulate, A. J. Lavery, and M. Schröder, *J. Chem. Soc., Chem. Commun.*, 1987, 118; A. J. Blake, A. J. Holder, T. I. Hyde, and M. Schröder, *ibid.*, p. 987; G. Reid, A. J. Blake, T. I. Hyde, and M. Schröder, *ibid.*, 1988, 1397.
- 22 A. J. Blake, G. Reid, and M. Schröder, *J. Chem. Soc., Dalton Trans.*, 1989, 1675.
- 23 E. J. Bounsall and S. P. Koprach, *Can. J. Chem.*, 1970, **44**, 1481; P. K. Bhattacharya, *J. Chem. Soc., Dalton Trans.*, 1980, 810; M. E. Sosa and M. L. Tobe, *J. Coord. Chem.*, 1987, **16**, 59.
- 24 DIRDIF, P. T. Beurskens, W. P. Bosman, H. M. Doesbury, Th. E. M. van den Hark, P. A. J. Prick, J. H. Noordik, G. Beurskens, R. O. Gould, and V. Parthasarathia, Applications of Direct Methods to Difference Structure Factors, University of Nijmegen, 1983.
- 25 DIFABS, Program for Empirical Absorption Corrections, N. Walker and D. Stuart, *Acta Crystallogr., Sect. A*, 1983, **39**, 158.
- 26 SHELX 76, Program for Crystal Structure Determination, G. M. Sheldrick, University of Cambridge, 1976.
- 27 ORTEP II, interactive version. P. D. Mallinson and K. W. Muir, *J. Appl. Crystallogr.*, 1985, **18**, 51.
- 28 CALC, Fortran77 version. R. O. Gould and P. Taylor, University of Edinburgh, 1985.
- 29 D. T. Cromer and J. L. Mann, *Acta Crystallogr., Sect. A*, 1968, **24**, 321.

Received 29th June 1990: Paper 0/02929G